Published in final edited form as:
Dev Dyn. 2009 October ; 238(10): 2688–2700. doi:10.1002/dvdy.22089.

Altered Hypoxia-inducible factor-1 alpha expression levels correlate with coronary vessel anomalies

Jamie Wikenheiser[1,2,*], **Julie A. Wolfram**[4,5], **Madhusudhana Gargesha**[3], **Ke Yang**[1], **Ganga Karunamuni**[1,2], **David L. Wilson**[3], **Gregg L. Semenza**[8], **Faton Agani**[2], **Steven A. Fisher**[7], **Nicole Ward**[4,6], and **Michiko Watanabe**[1]

[1] Department of Pediatrics, Rainbow Babies & Children's Hospital, 2101 Adelbert Road, Case Western Reserve University, Cleveland, OH, 44106-6011

[2] Department of Anatomy, Case Western Reserve University, 11100 Euclid Avenue, Cleveland, OH, 44106-6011

[3] Department of Biomedical Engineering, Case Western Reserve University, 11100 Euclid Avenue, Cleveland, OH, 44106-6011

[4] Department of Dermatology, Case Western Reserve University, 11100 Euclid Avenue, Cleveland, OH, 44106-6011

[5] Department of Pathology, Case Western Reserve University, 11100 Euclid Avenue, Cleveland, OH, 44106-6011

[6] Department of Neuroscience, Case Western Reserve University, 11100 Euclid Avenue, Cleveland, OH, 44106-6011

[7] Department of Medicine, Case Western Reserve University, 11100 Euclid Avenue, Cleveland, OH, 44106-6011

[8] Vascular Program, Institute for Cell Engineering, Departments of Pediatrics, Medicine, Oncology, Radiation Oncology, and McKusick-Nathans Institute of Genetic Medicine, The Johns Hopkins University School of Medicine, Baltimore, MD 21205

Abstract

The outflow tract myocardium and other regions corresponding to the location of the major coronary vessels of the developing chicken heart, display a high level of hypoxia as assessed by the hypoxia indicator EF5. The EF5 positive tissues were also specifically positive for nuclear-localized hypoxia inducible factor-1 alpha (HIF-1α), the oxygen-sensitive component of the hypoxia inducible factor-1 (HIF-1) heterodimer. This led to our hypothesis that there is a "template" of hypoxic tissue that determines the stereotyped pattern of the major coronary vessels. In this study we disturbed this template by altering ambient oxygen levels (hypoxia 15%; hyperoxia 75-40%) during the early phases of avian coronary vessel development, in order to alter tissue hypoxia, HIF-1α protein expression and its downstream target genes without high mortality. We also altered HIF-1α gene expression in the embryonic outflow tract cardiomyocytes by injecting an adenovirus containing a constitutively active form of HIF-1α (AdCA5). We assayed for coronary anomalies using anti-alpha-smooth muscle actin immunohistology. When incubated under abnormal oxygen levels or injected with a low titer of the AdCA5, coronary arteries

Corresponding author: Dr. Michiko Watanabe, Department of Pediatrics, Rainbow Babies and Children's Hospital, 2101 Adelbert Road, Cleveland, OH 44106-6011, Phone 216-844-7361, Fax 216-844-7642, mxw13@po.cwru.edu.
Current Address: Dr. Jamie C. Wikenheiser, Department of Pathology and Laboratory Medicine, David Geffen School of Medicine at the University of California, Los Angeles, 10833 Le Conte Avenue, Room 63-127C CHS, Los Angeles, CA 90095-1732, Phone 310-825-8761, jwikenheiser@mednet.ucla.edu

displayed deviations from their normal proximal connections to the aorta. These deviations were similar to known clinical anomalies of coronary arteries. These findings indicated that developing coronary vessels may be subject to a level of regulation that is dependent on differential oxygen levels within cardiac tissues and subsequent HIF-1 regulation of gene expression.

Introduction

The major coronary vessels form a stereotyped pattern that is consistent within a species and across species with four chambered hearts. The major vessels travel along sulcus regions with left and right attachments of the coronary arteries to the aorta. It was the goal of our study to investigate the mechanisms that produce this pattern.

The bulk of cells that contribute to the coronary vasculature (endothelial, fibroblasts, smooth muscle and pericytes) are supplied by the proepicardium, a transitional structure located posterior to the septum transversum, and the embryonic epicardium (Mikawa and Fischman, 1992; Mikawa and Gourdie, 1996). The cells of the proepicardial organ (PEO) form the embryonic epicardium and the mesothelial cells undergo an epithelial-mesenchymal transition (EMT). Angioblasts delivered by the proepicardium coalesce to form vesicles comprised of endothelial cells between stages 23–26 in chicken. These endothelial vesicles then coalesce to form nascent coronary vessels beginning at stage 27 (~ED 11.5 in mice) and attach to the systemic circulation by stage 32 (reviewed in Olivey et al., 2004). Angioblasts migrate into the epicardial matrix and myocardium and assemble into vascular tubes. These tubes form a capillary-like network (peritruncal ring) surrounding the base of the outflow tract and portions of this network fuse and penetrate the aorta, recruit smooth muscle cells, and the end result is two main coronary artery stems connecting the aorta to the coronary circulation (Bogers et al., 1989; Waldo et al., 1990; Reese et al., 2002 and Tomanek et al., 2005). The proximal segment of the coronary arteries develops by endothelial ingrowth from the peritruncal ring rather than by endothelial outgrowth from the aorta (Bogers et al., 1989; Waldo et al., 1990; Ando et al., 2004) and are invariably located at the same sites relative to the aortic leaflets. What allows the coronary vessels to develop in a similar architectural pattern from within and across species is still largely unknown.

Tissue hypoxia is a factor that has been identified as being critical to normal vascular development. Passive diffusion of oxygen and nutrients becomes limiting due to rapid cellular proliferation in developing embryos. These responses to decreased oxygen levels, or hypoxia, are required for normal development and patterning of the cardiovascular system (Ramirez-Bergeron and Simon, 2001). Hypoxia is also an essential physiological and developmental stimulus that plays a key role in the pathophysiology of cancer, heart attack, stroke and other major causes of mortality (Iyer et al., 1998). Hypoxia is also responsible for the activation of a number of genes which are important for cellular and tissue adaptation to low oxygen conditions and many of these responses are mediated through hypoxia-inducible factor 1 (HIF-1) (Semenza, 2001 and Dery et al., 2005).

HIF-1 was originally identified by its binding to a hypoxia response element (HRE) in the human erythropoietin (EPO) gene that was required for transcriptional activation in response to reduced cellular O_2 concentration (Semenza and Wang, 1992). HIF-1 is a heterodimer consisting of a constitutively expressed HIF-1β subunit and an O_2-regulated HIF-1α subunit (Wang et al., 1995). Under hypoxic conditions, hydroxylation of proline residues 402 and 564 and asparagine residue 803 in HIF-1α regulates protein stability and transactivation functions in an O_2-dependent manner (Huang et al., 1998; Lando et al., 2002). HIF-1α is then free to bind with HIF-1β in the nucleus and forms the HIF-1 transcription complex. The heterodimer can then bind to HRE-containing promoter regions in genes that can promote angiogenesis, glucose metabolism, cell survival and erythropoietin synthesis among other

functions (Livingston and Shivdasani, 2001; Semenza, 2003; Dery et al., 2005). HRE's are functionally essential HIF-1 binding sites with the consensus sequence 5′-RCGTG-3′ (Semenza et al., 1996).

Since the discovery of HIF-1, more than 70 genes have been found to be induced by HIF-1 (Semenza, 2004). HIF-1 and its family members play crucial roles in sensing changes in tissue oxygen tension and stimulating gene expression changes that enhance blood vessel growth into hypoxic tissues during post-gastrulation development (Ryan et al., 1998). HIF-1α is known to be required for normal cardiac morphogenesis (Compernolle et al., 2003; Krishnan et al., 2008). HIF-1α$^{-/-}$ mice die by ED 10.5 and exhibit dilated vasculature, hyperplastic myocardium, neural tube defects and cephalic mesenchymal cellular death (Iyer et al., 1998; Ryan et al., 1998; Kotch et al., 1999). Conditional deletion of HIF-1α from ventricular cardiomyocytes (MLC2v-cre) at an early stage leads to dysmorphogenesis and early lethality (E11-12) (Krishnan et al., 2008) and a less complete deletion in the same cells resulted in a modest but significant reduction of vessel counts in the myocardium compared with controls (Huang et al., 2004).

We showed that when the hypoxia marker EF5 [2-(2-nitro-1H-imidazol-1-yl)-N-(2,2,3,3,3-pentafluoropropyl) acetamide] (Koch, 2002) was injected into the vitelline vein of the chicken embryo *in ovo*, highly positive hypoxic regions were identified that included areas that corresponded to where the anastomosing peritruncal network of vessels around the base of the outflow tract (OFT) and the major coronary vessels develop (Sugishita et al., 2004A, B; Wikenheiser et al., 2006; Barbosky et al., 2007; Xu et al., 2007). These areas included the OFT myocardium, atrioventricular junction (AVJ), and the anterior/posterior interventricular sulcus where the anterior and posterior interventricular (AIV/PIV) vessels develop respectively. Furthermore, detection of nuclear-localized HIF-1α indicated that HIF-1 transcriptional activity is likely to be upregulated at these same EF5-positive sites. Comparison of staining patterns of the hypoxia indicator, nuclear-localized HIF-1α, vessel markers, and HIF-1-responsive gene expression led to the hypothesis that hypoxia and the consequent HIF-1α-regulated transcriptional responses are important for formation and organization of vessels in the early embryo. The co-localization of EF5 and HIF-1α nuclear staining patterns suggested that the levels of hypoxia we are detecting with EF5 within the myocardium are physiologically significant, and the differentially hypoxic myocardium may provide a template for coronary vessel organization by mobilizing HIF-1 transcriptional activity (Wikenheiser et al., 2006). The hypothesis tested is that differential levels of micro-environmental hypoxia within the embryonic myocardium regulate steps in coronary vessel development through HIF-1 transcriptional activation and its downstream genes. Regulating HIF-1 expression by altering ambient oxygen or through the use of an adenovirus carrying the gene for a constitutively active form of HIF-1α, we expected to disrupt the naturally occurring hypoxia template and downstream activity of HIF-1, resulting in altered patterns of the coronary vasculature.

Experimental Procedures

Preparation of Chicken Embryos

Fertile White Leghorn (Gallus gallus) chicken eggs were obtained from Case Western Reserve University's Squire Valleevue Farm (Cleveland, OH). Eggs were incubated in a humidified room air incubator at 38°C until the embryos reached appropriate stages for each experiment (Hamburger and Hamilton, 1951; HH 25-35 [ED 4.5-9]). From stage 25, embryos were either left at normoxic conditions (20.8% O_2), or subjected to hypoxic (15% O_2) and hyperoxic (75-40% O_2) conditions within a modified styrofoam chamber (Hova-Bator, G.Q.F. Mfg. Co., Savannah, GA) with O_2 percentage measured by an oxygen

regulator (PROOX 360 oxygen regulator; BioSpherix, Redfield, NY) connected to a nitrogen or oxygen tank.

We used an oxygen regulator for controlled oxygen levels and optimized conditions for effects on HIF-1 transcription while increasing survival of the embryos. We chose the ambient oxygen concentrations for our experiments based on preliminary and published data from our laboratory and others. Embryos had a high mortality rate (~50%) when exposed to 7.5% oxygen or less for longer than 6 hours. In contrast, embryos incubated at 12% O_2 have a better survival rate (~90–95%) even up to 24 h of exposure. Differences in EF5 staining within hypoxic, normoxic & hyperoxic tissue have been shown in embryonic rats from ED9-11. Even under 45% O_2, embryos stained with EF5 at these early stages were positive (Chen et al., 1999). This is the reason we decided to expose similar staged chicken embryos to 75% O_2 during its known highest hypoxia levels (ED 4.5-6.5) and then adjust to 40% thereafter (ED 6.5-9) to increase survival rates.

Our goal was to disturb the naturally occurring hypoxic template where coronary vessels develop by exposing embryos from stages 25–35 to 15% ambient oxygen. These conditions were chosen to allow survival while maximizing exposure to hypoxic conditions during stages of coronary vascular development. Under both hypoxic and hyperoxic regimens we had a survival rate between 95–98%. These stages span the time when a hypoxic myocardium is first detected by EF5 (stage 25; Sugishita et al., 2004A) and where angioblast/endothelial cells begin to coalesce and form early vessels (stage 27–32). Tissues were harvested at stages 27, 30 and 33, and then analyzed for protein expression for HIF-1α, VEGF-A, VEGFR2, Phosho-VEGFR2 (Tyr 1175), PDGF-B, Ang2 and Tie2 using the Western blotting technique. Stage 30 (unless otherwise noted) was selected for detection of proteins that are known to be HIF-1 regulated because it is the peak of hypoxia in the embryonic heart and it is also a full day before the coronaries connect to the aorta.

Adenovirus injections

Replication-defective recombinant adenoviruses were constructed as previously described (Kelly et al., 2003; Patel et al., 2005). AdCA5 contains a dual CMV promoter that drives expression of enhanced green fluorescent protein (GFP) and a constitutively active form of human HIF-1α (CA5) that contains a deletion of the oxygen-dependent domain (residues 392-520) and two missense mutations (Pro567Thr and Pro658Gln). These deletions and substitutions inhibit degradation of the HIF-1α protein under non-hypoxic conditions. Injection of adenovirus bearing the GFP sequence driven by the CMV promoter was used for the negative control. A total of 0.5 μl of adenovirus (5×10^7 pfu/ml)/0.5 μl PBS solution was injected into the pericardial space surrounding the heart at stage 17/18 (ED 2.5) as previously described (Fisher and Watanabe, 1996; Fisher et al., 1997; Watanabe et al., 1998). We used a lower titer than previously used (10^{14}, Sugishita et al., 2004B; Liu and Fisher, 2008) to mimic the levels achieved by mild hypoxia and to prevent gross structural defects in the OFT. Embryos were incubated to the appropriate stages and their tissues harvested and examined at stage 30–33 (ED 6.5-8).

Experiments involving the injection of plasmid DNA encoding a HIF-1α/VP16 fusion protein has also been shown to upregulate multiple angiogenic factors those of which include VEGF and angiopoietin-2 (Yamakawa et al., 2003), stimulates the recovery of blood flow in operative models of hindlimb ischemia (Vincent et al., 2000) and enhances angiogenesis in an acute myocardial infarction (Shyu et al., 2002). This plasmid DNA is similar to the structure of the constitutively active HIF-1α we used where the oxygen-dependent domain of HIF-1 is altered.

Immunohistology

Embryos were fixed in fresh 4% paraformaldehyde at 4°C for 1 hr, prepared for cyrosection through a series of sucrose solutions, frozen and sectioned in either the frontal or transverse plane. The 10–12 μm thick sections were collected on treated (Plus, Fisher) slides and immunostained. The primary antibodies anti-HIF-1α (Gift of Dr. Faton Agani), anti-α-smooth muscle actin conjugated with Cy3 (Sigma, St Louis, MO) and anti-VEGFR2 (Gift from Dr. Anne Eichmann) were incubated overnight at 4°C at a dilution of 1:500, 1:400 and no dilution respectively. Anti-HIF-1α and anti-VEGFR2 were detected with goat anti-rabbit IgG and goat anti-mouse IgG secondary antibodies respectively, conjugated with biotin (Vector, Burlingame, CA) at 1:200 dilution, and the signal was amplified with the TSA systems with fluorescein tyramide signal (Perkin Elmer, Boston, MA) per manufacturers instructions. Stained sections were observed with an inverted fluorescence microscope (Nikon Diaphot 200, Japan) or stereomicroscope (Leica MZ16F, Leica Microsystems, Wetzlar, Germany) and images were captured with a Q-Imaging Retiga EXi FAST 1394 digital camera and Q-capture software (Q-Imaging Burnaby, BC, Canada). Digital images were adjusted with Adobe Photoshop 7.0.1 software. Negative control images were captured with the same exposure as experimental images at the same magnification and adjusted in parallel.

Western blots

Staged embryonic chicken wholehearts were homogenized with a sonicator under ice within an ice-cold lysis buffer [50 mM Tris-HCl (pH 7.4), 150mM NaCl, 1% NP-40, 1% Triton X-100, 0.25% Na-deoxycholate, 0.1% SDS, 1 mM EDTA, and a protease inhibitor cocktail (Complete Mini, EDTA-free tablets (Roche, Mannheim, Germany)] and stored in a −80°C freezer until needed. Protein concentration was determined by using the DC protein assay (Bio-Rad Laboratories Inc, Hercules, CA). A total of 100 μg (50μg for VEGFR2, PDGF-B, Ang2 and Tie2) of the whole heart protein lysate was electrophoresed on either an 8% (HIF-1α, VEGFR2, Ang2 and Tie2) or 12% (PDGF-B) SDS-PAGE gel and then transferred onto a polyvinylidene difluoride (PVDF) membrane (Millipore, Bedford, MA). Membranes were blocked for 1 hour at room temperature with 5% nonfat milk in Tris-buffered saline with 1% Tween (TBST) (5% BSA in 1x TBST for Phospho-VEGFR2). The primary antibodies rabbit polyclonal anti-HIF-1α (Gift of Dr. Faton Agani), rabbit polyclonal anti-VEGFR2 (Santa Cruz Biotechnology, Inc, Santa Cruz, CA), rabbit polyclonal anti-PDGF-B (Santa Cruz Biotechnology, Inc), rabbit polyclonal anti-Ang2 (Santa Cruz Biotechnology, Inc), rabbit polyclonal anti-Tie2 (Santa Cruz Biotechnology, Inc) and monoclonal mouse anti-β-tubulin (Sigma, St Louis, MO) were incubated at a dilution of 1:500 (HIF-1α, VEGFR2, PDGF-B and Ang2) 1:1,000 (Tie2) and 1:100,000 (β-tub) respectively overnight at 4°C. The monoclonal antibody anti-β-tubulin was used for the loading control. After washing, the blots were incubated with an anti-rabbit IgG (H&L) HRP-linked antibody (Cell Signaling, Beverly, MA) for 1 hour at room temperature at a dilution of 1:5,000 (HIF-1α, VEGFR2, PDGF-B and Ang2) and 1:15,000 (Tie2). Anti-mouse IgG (H&L) HRP-linked antibody (Cell Signaling, Beverly, MA) was used against β-tubulin at a dilution of 1:100,000 for 1 hr at room temperature. Signals were then detected using an enhanced chemiluminescence detection system (ECL) (Pierce Chemical Co., Rockford, IL).

Immunoprecipitation was performed for Phospho-VEGFR2. Briefly, 100 μg of total protein lysate was incubated with 10 μl of primary antibody and 1 ml of lysis buffer containing protease inhibitors (as above) for 2 hours at 4°C. 100 μl of sepharose-A beads (GE Healthcare, Uppsala, Sweden) were added immediately after to the total solution and incubated overnight at 4°C. After the overnight incubation, samples were spun, supernatant was removed, and the remaining pellet was washed 3 times with lysis buffer. After the wash, 25 μl of 2x sample buffer (Bio-Rad Laboratories Inc, Hercules, CA) was added to each

sample and boiled for 10 minutes at about 100°C. Standard Western blot analysis was carried out on the boiled samples substituting BSA instead of milk for the blocking buffer. The primary antibody anti-Phospho-VEGFR2 (Cell Signaling, Beverly, MA) was incubated at a dilution of (1:2,500) overnight at 4°C. Anti-rabbit IgG (H&L) HRP-linked antibody (Cell Signaling, Beverly, MA) for 1 hour at room temperature at a dilution of (1:15,000) was used as the secondary antibody. Signals were then detected using an enhanced chemiluminescence detection system as described above.

Enzyme-Linked Immunosorbent Assay (ELISA)

VEGF protein of stage 30 whole-hearts from control, hypoxic and hyperoxic treated embryos ($n = 4$) were detected by ELISA (QuantiGlo, R&D Systems, Minneapolis, MN). Aliquots of pooled hearts from 6 separate incubations were homogenized in the same ice-cold lysis buffer as with the Western blot assays described above. A six-point VEGF standard curve was used, which consisted of recombinant human $VEGF_{165}$ at concentrations of 0–20,000 pg/ml.

3D Imaging of coronary trunks

3D imaging using AMIRAR software (Visage Imaging, Carlsbad, CA) was used to confirm what was observed earlier with stained serial sections 12 μm thick. Consecutive α-smooth muscle actin stained sections (40–48 in total) from 10–12 slides were used to render a 3D reconstruction in the transverse plane near the aorta. The resulting image could be rotated to analyze the anomaly at different angles.

Statistical analysis

Data are presented as mean ± standard error of the mean. Statistical comparisons among groups were made using a two-tailed Student-t test. A $p < 0.05$ was considered statistically significant.

Results

HIF-1α nuclear localization in embryonic myocardium

The increase in the frequency of HIF-1α-positive nuclei as assayed by immunofluorescence staining of cryosections was consistent with the increase in protein expression levels as assessed by Western Blot analysis at all stages and oxygen regimens. An unexpected finding was that under both hyperoxia regimens, the 75-40% O_2 and 40% O_2 for 4.5 days (40% only data not shown), the immunostaining pattern consistently supported an increase in the number of HIF-1α positive nuclei compared to normoxic levels. Nuclear-localized staining was increased under the hypoxic regimen in regions of the outflow tract, atrioventricular junction and interventricular septum, but only slightly increased after the hyperoxic treatment in these same regions at stages 27 and 30. The staining of stage 33 embryo hearts after hyperoxic treatment was near normoxic levels in these same regions (Figure 1).

Transverse sections at stage 30 (ED 6.5) near the left and right coronary attachments of the outflow tract showed HIF-1α expression differences. Under normoxic conditions, only a discrete group of cells that were positive for nuclear-localized HIF-1α staining were present in the region where the left and right coronaries attach to the aorta. There was a dramatic increase in the number of cells found in that region with HIF-1α nuclear staining under either the hypoxic or hyperoxic regimens with the hypoxic regimen resulting in a wider region of HIF-1α nuclear staining compared to the hyperoxic regimen at stage 30 (Figure 2).

HIF-1α and downstream protein expression levels

When embryos were subjected to a regimen of 15% O_2 for 4.5 continuous days, HIF-1α protein expression as assessed by Western blot analysis was increased at stage 27, 30 and 33 by an average of 4.52, 3.63 and 1.65 fold respectively ($n = 6$). Stage 27 and 30 but not stage 33 extracts, were significantly increased in HIF-1α protein expression under hypoxia ($p = 0.009$; $p = 0.005$ respectively). Consistent with the immunohistology results, under the hyperoxic regimen of 75% O_2 for 2 days followed by 40% O_2 for the remaining 2.5 days, HIF-1α protein expression was increased by an average of 1.55, 1.80 and 0.313 fold respectively ($n = 4$), with stage 30 extracts showing a significant increase ($p = 0.03$) (Figure 3A).

The ELISA assays indicated that VEGF-A protein expression at stage 30 increased significantly under both hypoxic ($p = 0.003$; $n = 4$) and hyperoxic ($p = 0.002$; $n = 4$) regimens (Figure 3B). With Western blots, we measured whole VEGFR2 and a specific phosphorylated VEGFR2 residue that has been found to be essential for endothelial and hematopoietic development during embryogenesis (Sakuri et al., 2005) and found both are significantly increased under hypoxia ($p = 0.01$; $n = 4$) but not with our hyperoxia regimen at stage 30 (Figure 3C). This tyrosine residue is phosphorylated at 1175 in human, 1173 in mouse and 1168 in chicken. The increase in phosphorylated VEGFR2 was dependent on the overall increase in VEGFR2 and could represent an increase in the number of EC's, receptors on the EC's or both, and may be attributed to an increase in VEGFR2 expression in cardiomyocytes of the distal OFT.

Platelet-derived growth factor-B (PDGF-B) which is specific to vascular endothelial cells is a known mitogen for smooth muscle cells and pericytes and has been shown to be active during chicken coronary development (Van den Akker et al., 2005). PDGF-B protein expression levels under our hypoxia and hyperoxia regimens increased significantly at stage 30 ($p = 0.02$ and $p = 0.01$ respectively; $n = 4$) (Figure 3D).

Angiopoietin-2 (Ang2) and the angiopoietin receptor Tie2 at stage 30 levels increased but not significantly under the hypoxia and hyperoxia regimens. At stage 33, just after the left and right coronary arteries attach to the aorta, Ang2 protein levels were increased but still not to a significant level under hypoxic conditions ($n = 4$) (Figure 3E, F). A significant increase in Tie2 protein expression was observed at stage 33 ($n = 4$) under both the hypoxic and hyperoxic regimens ($p = 0.01$ and $p = 0.01$ respectively) (Figure 3G). Tie2 has not been found to be a downstream target of HIF-1α, but we chose to investigate it because it is important for the regulation of endothelial cell differentiation during vascular remodeling and maturation.

In summary, the expression of HIF-1 downstream target genes important in vascular development such as VEGF-A, VEGFR2 and PDGF-B, increased to significant levels after exposure to altered ambient oxygen levels. Ang2 levels increased but not to significant levels. A non-HIF-1α target gene, the Tie2 receptor, increased significantly only after the connection of the left and right coronary arteries to the aorta. These data indicate that the hypoxic and hyperoxic regimens we used altered HIF-1α activity during the establishment of the coronary circulation, to a level that lead to the mis-regulation of important proteins associated with vascular differentiation and maturation.

Altered HIF-1α expression by hypoxia and hyperoxia coincides with left and right coronary artery anomalies

Transverse sections near the coronary artery attachments of stage 35 embryos were stained with anti-α-smooth muscle actin directly labeled with Cy3 in order to locate the larger coronary vessels that are invested with smooth muscle cells. Under mildly hypoxic

conditions (15% ambient oxygen) for 4.5 days (stages 25–35/ED 4.5 to 9), 90% (9/10) of the embryos had anomalies of the proximal coronary vessels at stage 35 compared to normoxic control samples ($n = 10$). The majority of the anatomical anomalies were observed in the right coronary vessel (7/10). The left coronary variations occurred 5 out of 10 times. Simultaneous left and right coronary variations occurred in 4 out of 10 embryos. The anatomical anomalies resulting under hypoxic conditions included (1) double right coronaries originating at the right cusp; (2) proximal swelling at the right coronary stem; (3) the right coronary originating from the posterior cusp; (4) a retro-aortic coronary branch originating from the left coronary that wrapped around the aorta to fuse with the right coronary and posterior cusp; and (5) tortuous proximal regions of the left and right coronaries. Under the hyperoxic (75-40% ambient oxygen) regimen, 50% (5/10) of the embryos displayed anatomical variations and these anomalies were similar to those found in the embryos treated with the hypoxic regimen. These included the retro-aortic left coronary branch (4/5) and double right coronary coming off of the right cusp (Figure 4A–H and Table 1).

Three-dimensional reconstructions were used to verify the observed anomalies and revealed altered angles at branch points as well as abnormal trajectories of anomalous branches that were not easily detected with observations of individual stained sections (Figure 4I–L).

Over-expression of constitutively active HIF-1α (AdCA5) in the OFT myocardium resulted in coronary anomalies

To test whether these coronary anomalies could be due to alterations in HIF-1α function alone in local cardiomyocytes, we used engineered adenovirus infection. AdCA5 and AdGFP (used as the control adenovirus) injected embryos displayed GFP expression specifically within the myocardium at the base of the OFT as we observed previously using adenoviruses with other genes driven by the CMV promoter (Watanabe et al., 1998; Watanabe et al., 2001; Sallee et al., 2004). When embryos were injected with AdCA5 at stage 17/18 and analyzed at stage 33, 75% (6/8) exhibited coronary anomalies. We observed anomalies similar to that observed after exposure to hypoxic and hyperoxic regimens: retro-aortic coronaries attaching near the posterior cusp of the aorta, additional coronary stems lateral to the right coronary artery, a posterior cusp branch that coursed towards the main left coronary, and finally an embryo with no right coronary artery but displaying a retro-aortic branch off the left coronary that extended around the aorta and following the tract of the right coronary artery (Figure 5 and Table 1). The vehicle controls, AdGFP injected embryos, displayed no anomalies (0/8). No conotruncal defects or abnormal rotation involving the aorta and pulmonary trunk were observed with either the control or constitutively active HIF-1α injected embryos with a 5×10^7 titer. These results suggested that coronary anomalies could arise from overactive HIF-1 in cardiomyocytes alone. AdCA5 injected embryos also displayed more intense staining for VEGFR2 compared to AdGFP controls near sites of the left and right coronary attachments to the aorta at stage 30 (Figure 5D–F). The survival rates of the embryos injected with AdCA5 and AdGFP controls at stage 33 was 33% and 47% respectively.

In order to detect changes in coronary precursors at an earlier stage, we injected AdCA5 to quail embryos and assessed the condition of Qh-1+ cells at stage 32 which is the stage when coronary vessels begin to connect to the aortic lumen. Qh-1 is an antibody that detects hemangioblasts and angioblasts as well as endothelial cells in quail (Kattan et al., 2004). The numbers of individual Qh-1+ cells as well as the density of the vessel network at the base of the OFT near the GFP+ AdCA5-infected cells was increased (Figure 6 N–P). None of the Qh-1+ cells were GFP+, supporting the specificity of the adenovirus infection for the underlying cardiomyocytes.

Discussion

The tissues of the developing embryo are relatively hypoxic during normal development and, in fact, hypoxic conditions are required for normal development. A number of studies have demonstrated that hypoxia is required for patterning of the cardiovascular system, embryonic blood vessel formation, remodeling of the cardiac outflow tract and maturation of the conduction system (Chen et al., 1999; Ramirez-Bergeron and Simon, 2001; Lee et al., 2001; Sugishita et al., 2004A, B; Lampl, 2005; Nanka et al., 2008). However, it is clear that too high a level of hypoxia is detrimental to embryo survival and the effects of exposure to such levels vary with the stage of exposure. The effects of even mild-hypoxia exposure regimens can be stage dependent as well. Recently it was shown that exposure to 16% O_2 from ED 2-10 resulted in a 10% survival rate and coronary artery abnormalities at ED10 (Nanka et al., 2008). Our experiments targeted the stages of coronary vessel development ED 4.5-9 with 15% O_2 which resulted in a >95% survival rate at ED 9 and multiple coronary artery morphology abnormalities.

We observed particularly hypoxic regions of the heart under normoxic conditions using the hypoxia marker EF5 (Sugishita et al., 2004A; Wikenheiser et al., 2006). Embryonic heart tissue that displayed hypoxic regions of 0.1–10% O_2 (the range that EF5 detects) included the outflow tract, atrioventricular junction, and the regions that correspond to where the major coronary vessels develop. We hypothesized that these regions may serve as a “hypoxic template” for the patterning of the coronary arteries. In this study we altered this hypoxic template by varying ambient oxygen concentrations and over-expressing HIF-1α in the OFT cardiomyocytes through an adenovirus containing a constitutively active form of human HIF-1α (AdCA5). We determined that HIF-1α expression levels along with some important downstream vasculogenic and angiogenic factors such as VEGF-A, VEGFR2, PDGF-B, Ang2 and Tie2, changed significantly under these conditions and are likely to have contributed to the high frequency of coronary anomalies resulting from all three experimental manipulations. Coronary artery anomalies have also been described when FGF-2 and/or PDGF were inhibited (Tomanek et al., 2008).

Similar anomalies after hypoxia, hyperoxia, and constitutively active HIF-1α exposure

It has been established that proximal coronary arteries develop by endothelial ingrowth rather than an outgrowth from the aortic lumen (Bogers et al., 1989; Waldo et al., 1990; Ando et al., 2004). A capillary network (peritruncal ring) surrounds the base of the outflow tract in epicardium and studies have supported that this network initially penetrates the myocardium and connects to the aorta at multiple sites in avian embryos (Waldo et al., 1994; Ando et al., 2004). After final remodeling only two attachments persist, recruit smooth muscle cells some of neural crest origin, and form the two main coronary arteries. Our findings were that hypoxic, hyperoxic, or overactive HIF-1 resulted in extra coronary arteries and attachments some in ectopic sites. These may have arisen from the persistence of the immature coronary endothelial strands that would normally have regressed. Their persistence may have been due to the increase in HIF-1 activity and upregulation of downstream genes such as VEGF (reviewed in Jiang and Liu, 2008; Witmer et al., 2003) that may have increased precursor recruitment and/or survival to maintain nascent vessels at ectopic sites. VEGF family members have been shown recently to play a critical role in the formation of coronary ostia (Tomanek et al., 2006A, Tomanek et al., 2006B). VEGF and the VEGFR/Akt signaling pathway have been proposed to serve in survival of endothelial cells (reviewed in Breen 2007), neurons (Zachary, 2005), and OFT cardiomyocytes (reviewed in Sugishita et al., 2004C; Liu and Fisher 2008). Alternatively, the abnormal coronary pattern could have resulted from an earlier defect, the recruitment of epicardial vascular precursors to ectopic sites and/or their overproliferation and survival. Our findings support this

possibility. We observed increased numbers of Qh-1+ cells and vessels at the base of the OFT after AdCA5 infection (Figure 5N–P).

Local myocardial paracrine control over coronary vessel patterns

Our previous studies have demonstrated that the method of application of recombinant adenovirus by itself does not perturb cardiac morphologies and that the exogenous protein is preferentially expressed in outflow tract cardiomyocytes adjacent to the conoventricular junction (Fisher and Watanabe, 1996; Fisher et al., 1997; Watanabe et al., 1998). We were able to reproduce the coronary anomalies induced by the hypoxia/hyperoxia regimens after infection by the adenovirus containing a constitutively active form of HIF-1α (AdCA5). The over-expression of HIF-1α through AdCA5 resulted in a high rate (75%) of proximal coronary anomalies near the aorta. There was no other obvious heart defects likely due to the low titer of adenovirus (5×10^7) used. HIF-1 has been shown to function cell-autonomously in endothelial cells (Ramirez-Bergeron et al., 2006; Licht et al., 2006), but our results indicate that altering HIF-1α levels in a discrete region of OFT cardiomyocytes alone results in coronary anomalies similar to that induced by whole embryo exposure to hypoxic and hyperoxic conditions. Therefore a non-cell autonomous effect of HIF-1 transcription in the adjacent myocardium may by itself influence coronary endothelial cell precursor recruitment and/or survival and may be the dominant signal that causes the anomalies when the whole embryo is exposed to hypoxic and hyperoxic conditions.

The non-cell autonomous control of HIF-1 on coronary vessel formation has some support in studies where HIF-1α was deleted in mouse models. The conditional deletion of HIF-1α from ventricular cardiomyocytes (MLC2v-cre) at an early stage resulted in dysmorphogenesis and early lethality (E11-12) (Krishnan et al., 2008) and therefore had limited use in studying coronary vessel development. A less complete deletion targeting only the left ventricle resulted in a reduction of VEGF-A expression and a modest but significant reduction in vessel counts in the myocardium compared with controls but analysis of the proximal coronary vessel patterning was not undertaken in this study (Huang et al., 2004). Interestingly PDGF increased in these hearts. In comparison to our studies, the promoter used for this latter conditional deletion may not have allowed substantial deletion in the outflow tract cardiomyocytes adjacent to the proximal coronary vessels.

Effects of Hyperoxia

The increase in HIF-1α protein levels and in the number of cells with nuclear localized HIF-1α as well as increases in the level of some HIF-1 downstream genes under hyperoxic conditions was unexpected but recent data provides an explanation. Reactive oxygen species (ROS) that increase under hyperoxic conditions (Jamieson et al., 1986) may play a part in stabilizing HIF-1α protein. ROS generated at the Mitochondrial Complex III, along with cytochrome c activity have been found to help stabilize HIF-1α during hypoxia (Chandel et al., 2000; Turcotte et al., 2003; Brunelle et al., 2005; Guzy et al., 2005; Mansfield et al., 2005). This may explain why even a small increase in HIF-1α protein expression during hyperoxic conditions was enough to disturb the balance of multiple factors needed to form normal coronary attachments near the aorta. There is also accumulating evidence suggesting that ROS derived from NAD(P)H oxidase are involved in the induction of HIF-1α (Richard et al., 2000; Gorlach et al., 2001; Haddad and Land, 2001; Page et al., 2002; Yang et al,. 2003) and VEGF (Richard et al., 2000; Brandes et al,. 2002) in vascular cells. There are many studies showing that ROS can mediate VEGF-induced angiogenic effects including endothelial cell migration, proliferation and tube formation (Ushio-Fukai et al., 2002; Colavitti et al., 2002; van Wetering et al., 2002; Lin et al., 2003; Reviewed in Ushio-Fukai and Alexander, 2004). VEGF has been shown to be stimulated under hyperoxic conditions (Sheikh et al., 2000) in a wound model. Recently, ROS has also been found to be a critical

mediator of coronary collateral development in the canine model (Gu et al., 2003). These findings suggest that hyperoxia may be able to alter HIF-1 activity transcriptionally as well as post-transcriptionally and may directly affect VEGF expression as well. Thus, the response of the embryonic tissues to an increase in ROS under either hypoxic or our hyperoxic regimens may partially explain why both HIF-1α and VEGF protein expression increased in our studies under both regimens. The combination of HIF-1α and VEGF over-expression under either regimen may also explain the similarity in the effect on the quality of the coronary anomalies.

3-D Analysis of Coronary Anomalies

We used 3D reconstructions of consecutive serial sections at the level of the proximal coronary arteries stained with α-smooth muscle actin to further analyze select anomalies. We discovered that the reconstructions allowed us to assess proximity of structures, angles and the trajectory of the anomalous branches that were not easily detected with 2-D analysis. For example, we discovered that some anomalous vessels observed in the experimentally treated embryos traveled closer to the base of the pulmonary trunk than in the controls. Although we did not measure flow in the anomalous vessels, the altered angles and trajectories of the branches are likely to change fluid dynamics of coronary blood flow within the heart. We found no appreciable differences in lumen diameters with the experimental conditions except in specific sites of swellings. The coronary vessels seemed to have achieved maturation and were not abnormally small and irregular like vessels found in mice with elevated VEGF concentrations (Miquerol et al., 1999, 2000).

With stereomicroscopy, no significant increases or decreases were observed in the total number of larger distal coronary vessels after exposure to any one of the three treatments.

Coronary artery anomalies and their clinical correlation

In this study, exposure of avian embryos to a mild level of ambient oxygen (15%) that is similar to that experienced in Denver, Colorado (~17%), leads to abnormal coronary artery patterning. While we do not know if the particular anomalies we induced have long term consequences for the chickens after hatching, we deduced that the structure of the anomalies have the potential to alter fluid dynamics within the proximal coronaries and may predispose to future pathology. The anomalies included swellings, tortuosities, altered angles, extra attachments of coronary stems at the right and left cusps, and attachments at the wrong posterior cusp,

Human fetal oxygen tensions normally are 20 to 30 % of that of adults (Longo, 1976), and can be reduced further by the mother smoking, living at high altitude, or being exposed to environmental pollution such as carbon monoxide. Maternal smoking induces fetal hypoxia and morphological changes in the placenta that increases the risks of intrauterine growth retardation and placental abruption that in turn may cause late fetal death and possibly neonatal mortality (Cnattingius and Nordstrom, 1996). In utero hypoxia exposure induced by smoking and other conditions is also linked by epidemiological studies and by studies of animal models to adult onset cardiovascular disease (Zhang, 2005). We propose that some of the negative consequences of in utero exposure to hypoxia might be explained by the presence of anomalous coronary vessels that may not manifest pathology until later in life.

The exposure of human embryos to mildly hypoxic conditions at a critical time during their development may be enough to induce, as in our avian embryos, alterations in the pattern of coronary arteries. While many coronary anomalies are believed to have no negative consequences, certain congenital coronary anomalies such as anomalous left coronary from the pulmonary artery (ALCAPA) or opposite sinus (ACAOS) have been associated with

exercise-related deaths (Taylor et al., 1992; Angelini, 2007). These defects are usually not detected until an autopsy is performed after an exercise related death (Frescura et al., 1998; Eckart et al., 2006). Understanding how they develop and anticipating their presence is important for clinical considerations (Angelini, 2007).

Summary

Alteration of the "hypoxic template" by manipulating HIF-1α levels may result in maintaining coronaries at the wrong insertion point and creating the extra branches and tracts that were induced in this study. The anomalies may be compatible with life but some are likely to alter blood flow patterns and may increase susceptibility to coronary artery disease later in life. Our manipulation of the levels of HIF-1α during specific stages of embryonic development has allowed us to reveal a novel role for HIF-1α in coronary artery pattern development.

Acknowledgments

The authors thank Dr. Oleg Kolevanko of Rainbow Babies and Children's Hospital for his clinical assessment of the observed anatomical anomalies in chicken embryos and Dr. Hongbin Liu for her advice on adenovirus injections. We also thank Yong Qiu Doughman for her excellent technical assistance in many aspects of these studies. Supported in part by NIH Grants HL65314, HL0775436 and ES103507.

References

1. Ando K, Nakajima Y, Yamagishi T, Yamamoto S, Nakamura H. Development of proximal coronary arteries in quail embryonic heart: Multiple capillaries penetrating the aortic sinus fuse to form main coronary trunk. Circ Res. 2004; 94:346–352. [PubMed: 14684625]
2. Angelini P. Coronary artery anomalies: An entity in search of an identity. Circulation. 2007; 115:1296–1305. [PubMed: 17353457]
3. Barbosky L, Lawrence DK, Karunamuni G, Wikenheiser JC, Doughman YQ, Visconti RP, Burch JB, Watanabe M. Apoptosis in the developing mouse heart. Dev Dyn. 2006; 235:2592–2602. [PubMed: 16881058]
4. Bogers AJJC, Gittenberger-de Groot AC, Poelmann RE, Peault BM, Huysmans HA. Development of the origin of the coronary arteries, a matter of ingrowth or outgrowth? Anat Embryol. 1989; 180:437–441. [PubMed: 2619086]
5. Brandes RP, Miller FJ, Beer S, Haendler J, Hoffmann J, Ha T, Holland SM, Gorlach A, Busse R. The vascular NADPH oxidase subunit p47phox is involved in redox-mediated gene expression. Free Radic Biol Med. 2002; 32:1116–1122. [PubMed: 12031896]
6. Breen EC. VEGF in biological control. J Cell Biochem. 2007; 102:1358–1367. [PubMed: 17979153]
7. Brunelle JK, Bell EL, Quesada NM, Vercauteren K, Tiranti V, Zeviani M, Scarpulla RC, Chandel NS. Oxygen sensing requires mitochondrial ROS but not oxidative phosphorylation. Cell Metab. 2005; 1:409–414. [PubMed: 16054090]
8. Chandel NS, McClintock DS, Feliciano CE, Wood TM, Melendez JA, Rodriguez AM, Schumacker PT. Reactive oxygen species generated at mitochondrial complex III stabilize hypoxia-inducible factor-1α during hypoxia. J Biol Chem. 2000; 275:25130–25138. [PubMed: 10833514]
9. Chen EY, Fujinaga M, Giaccia AJ. Hypoxic microenvironment within an embryo induces apoptosis and is essential for proper morphological development. Teratology. 1999; 60:215–225. [PubMed: 10508975]
10. Cnattingius S, Nordstrom ML. Maternal smoking and feto-infant mortality: biological pathways and public health significance. Acta Paediatr. 1996; 85:1400–1402. [PubMed: 9001647]
11. Colavitti R, Pani G, Bedogni B, Anzevino R, Borrello S, Waltenberger J, Galeotti T. Reactive oxygen species as downstream mediators of angiogenic signaling by vascular endothelial growth factor receptor-2/KDR. J Biol Chem. 2002; 277:3101–3108. [PubMed: 11719508]

12. Compernolle V, Brusselmans K, Franco D, Moorman A, Dewerchin M, Collen D, Carmeliet P. Cardia bifida, defective heart development and abnormal neural crest migration in embryos lacking hypoxia-inducible factor-1 alpha. Cardiovasc Res. 2003; 60:569–579. [PubMed: 14659802]

13. Dery M-AC, Michaud MD, Richard DE. Hypoxia-inducible factor 1: regulation by hypoxic and non-hypoxic activators. Int J Biochem Cell Biol. 2005; 37:535–540. [PubMed: 15618010]

14. Eckart RE, Jones SO 4th, Shry EA, Garrett PD, Scoville SL. Sudden death associated with anomalous coronary origin and obstructive coronary disease in the young. Cardiol Rev. 2006; 14:161–163. [PubMed: 16788326]

15. Fisher SA, Watanabe M. Expression of exogenous protein and analysis of morphogenesis in the developing chicken heart using an adenoviral vector. Cardiovasc Res. 1996; 31:E86–95. [PubMed: 8681350]

16. Fisher SA, Siwik E, Branellec D, Walsh K, Watanabe M. Forced expression of the homeodomain protein Gax inhibits cardiomyocytes proliferation and perturbs heart morphogenesis. Development. 1997; 124:4405–4413. [PubMed: 9334288]

17. Frescura C, Basso C, Thiene G, Corrado D, Pennelli T, Angelini A, Daliento L. Anomalous origin of coronary arteries and risk of sudden death: a study based on an autopsy population of congenital heart disease. Hum Pathol. 1999; 29:689–695. [PubMed: 9670825]

18. Gu JW, Elam J, Sartin A, Li W, Roach R, Adair TH. Moderate levels of ethanol induce expression of vascular endothelial growth factor and stimulate angiogenesis. Am J Physiol Regul Integr Comp Physiol. 2001; 281:R365–372. [PubMed: 11404314]

19. Gu W, Weihrauch D, Tanaka K, Tessmer JP, Pagel PS, Kersten JR, Chilian WM, Warltier DC. Reactive oxygen species are critical mediators of coronary collateral development in a canine model. Am J Physiol Heart Circ Physiol. 2003; 285:H1582–H1589. [PubMed: 12816750]

20. Gorlach A, Diebold I, Schini-Kerth VB, Berchner-Pfannschmidt U, Roth U, Brandes RP, Kietzmann T, Busse R. Thrombin activates the hypoxia-inducible factor-1 signaling pathway in vascular smooth muscle cells: Role of the p22(phox)-containing NADPH oxidase. Circ Res. 2001; 89:47–54. [PubMed: 11440977]

21. Guzy RD, Hoyos B, Robin E, Chen H, Liu L, Mansfield KD, Simon MC, Hammerling U, Schumacker PT. Mitochondrial complex III is required for hypoxia-induced ROS production and cellular oxygen sensing. Cell Metab. 2005; 1:401–408. [PubMed: 16054089]

22. Haddad JJ, Land SC. A non-hypoxic, ROS-sensitive pathway mediates TNF-alpha-dependent regulation of HIF-1 alpha. FEBS Lett. 2001; 505:269–274. [PubMed: 11566189]

23. Hamburger V, Hamilton HL. A series of normal stages in the development of the chick embryo. J Morphol. 1951; 88:49–92.

24. Huang LE, Gu J, Schau M, Bunn HF. Regulation of hypoxia-inducible factor 1 alpha is mediated by an O_2-dependent degradation domain via the ubiquitin-proteasome pathway. Proc Natl Acad Sci USA. 1998; 95:7987–7992. [PubMed: 9653127]

25. Huang Y, Hickey RP, Yeh JL, Liu D, Dadak A, Young LH, Johnson RS, Giordano FJ. Cardiac myocyte-specific HIF-1 alpha deletion alters vascularization, energy availability, calcium flux, and contractility in the normoxic heart. FASEB J. 2004; 18:1138–1140. [PubMed: 15132980]

26. Iyer N, Kotch L, Agani F, Leung S, Laughner E, Wenger R, Gassmann M, Gearhart J, Lawler A, Yu A, Semenza GL. Cellular and developmental control of O_2 homeostasis by hypoxia-inducible factor 1α. Genes Dev. 1998; 12:149–162. [PubMed: 9436976]

27. Jamieson D, Chance B, Cadenas E, Boveris A. The relation of free radical production to hyperoxia. Annu Rev Physiol. 1986; 48:703–19. [PubMed: 3010832]

28. Jiang BH, Liu LZ. AKT signaling in regulating angiogenesis. Curr Cancer Drug Targets. 2008; 8:19–26. [PubMed: 18288940]

29. Kattan J, Dettman RW, Bristow J. Formation and remodeling of the coronary vascular bed in the embryonic avian heart. Dev Dyn. 2004; 230:34–43. [PubMed: 15108307]

30. Kelly BD, Hacket SF, Hirota K, Yuji Oshima, Cai Z, Berg-Dixon S, Rowan A, Yan Z, Campochiaro PA, Semenza GL. Cell type-specific regulation of angiogenic growth factor gene expression and induction of angiogenesis in nonischemic tissue by a constitutively active form of hypoxia-inducible factor 1. Circ Res. 2003; 93:1074–1081. [PubMed: 14576200]

31. Koch C. Measurements of absolute oxygen levels in cells and tissues using oxygen sensors and the 2-nitroimidazole EF5. Methods Enzymol. 2002; 352:3–31. [PubMed: 12125356]
32. Kotch LE, Iyer NV, Laughner E, Semenza GL. Defective vascularization of HIF-1α-null embryos is not associated with VEGF deficiency but with mesenchymal cell death. Dev Biol. 1999; 209:254–267. [PubMed: 10328919]
33. Krishnan J, Ahuja P, Bodenmann S, Snapik D, Perriard E, Krek W, Perriard J-C. Essential role of developmentally activated hypoxia-inducible factor 1a for cardiac morphogenesis and function. Circ Res. 2008; 103:1139–1146. [PubMed: 18849322]
34. Lampl M. Cellular life histories and bow tie biology. Am J Hum Biol. 2005; 17:66–80. [PubMed: 15611965]
35. Lando D, Peet DJ, Gorman JJ, Whelan DA, Whitelaw ML, Bruick RK. FIH-1 is an asparaginyl hydroxylase enzyme that regulates the transcriptional activity of hypoxia-inducible factor. Genes Dev. 2002; 16:1466–1471. [PubMed: 12080085]
36. Lee YM, Jeong CH, Koo SY, Son MJ, Song HS, Bae SK, Raleigh JA, Chung HY, Yoo MA, Kim KW. Determination of hypoxic region by hypoxia marker in developing mouse embryos in vivo: a possible signal for vessel development. Dev Dyn. 2001; 220:175–186. [PubMed: 11169851]
37. Licht AH, Muller-Holtkamp F, Flamme I, Breier G. Inhibition of hypoxia-inducible factor activity in endothelial cells disrupts embryonic cardiovascular development. Blood. 2006; 107:584–590. [PubMed: 16189264]
38. Lin MT, Yen ML, Lin CY, Kuo ML. Inhibition of vascular endothelial growth factor-induced angiogenesis by resveratrol through interruption of Src-dependent vascular endothelial cadherin tyrosine phosphorylation. Mol Pharmacol. 2003; 64:1029–1036. [PubMed: 14573751]
39. Lindahl P, Johansson BR, Leveen P, Betsholtz C. Pericyte loss and microaneurysm formation in PDGF-B-deficient mice. Science. 1997; 277:242–245. [PubMed: 9211853]
40. Liu H, Fisher SA. Hypoxia-inducible transcription factor-1 alpha triggers an autocrine survival pathway during embryonic cardiac outflow tract remodeling. Circ Res. 2008; 102:1331–1339. [PubMed: 18467628]
41. Livingston DM, Shivdasani R. Toward mechanism-based cancer care. JAMA. 2001; 285:588–593. [PubMed: 11176864]
42. Longo LD. Carbon monoxide: effects on oxygenation of the fetus in utero. Science. 1976; 194:523–525. [PubMed: 973133]
43. Mansfield KD, Guzy RD, Pan Y, Young RM, Cash TP, Schumacker PT, Simon MC. Mitochondrial dysfunction resulting from loss of cytochrome c impairs cellular oxygen sensing and hypoxic HIF-alpha activation. Cell Metab. 2005; 1:393–399. [PubMed: 16054088]
44. Mikawa T, Fischman DA. Retroviral analysis of cardiac morphogenesis: discontinuous formation of coronary vessels. Proc Natl Acad Sci USA. 1992; 89:9504–9508. [PubMed: 1409660]
45. Mikawa T, Gourdie RG. Pericardial mesoderm generates a population of coronary smooth muscle cells migrating into the heart along with ingrowth of the epicardial organ. Dev Biol. 1996; 174:221–232. [PubMed: 8631495]
46. Miquerol L, Gertsenstein M, Harpal K, Rossant J, Nagy A. Multiple developmental roles of VEGF suggested by a lacz-tagged allele. Dev Biol. 1999; 212:307–322. [PubMed: 10433823]
47. Miquerol L, Langille B, Nagy A. Embryonic development is disrupted by modest increases in vascular endothelial growth factor gene expression. Development. 2000; 127:3941–3946. [PubMed: 10952892]
48. Nanka O, Krizova P, Fikrle M, Tuma M, Blaha M, Grim M, Sedmera D. Abnormal myocardial and coronary vasculature development in experimental hypoxia. Anat Rec. 2008; 291:1187–1199.
49. Olivey HE, Compton LA, Barnett JV. Coronary vessel development: The epicarium delivers. Trends Cardiovasc Med. 2004; 14:247–257. [PubMed: 15451517]
50. Page EL, Robitalle GA, Pouyssegur J, Richard DE. Induction of hypoxia-inducible factor-1 alpha by transcriptional and translational mechanisms. J Biol Chem. 2002; 277:48402–48409.
51. Patel TH, Kimura H, Weiss CR, Semenza GL, Hofmann LV. Constitutively active HIF-1a improves perfusion and arterial remodeling in an endovascular model of limb ischemia. Cardiovasc Res. 2005; 68:144–154. [PubMed: 15921668]

52. Pardanaud L, Altmann C, Kitos P, Dieterlen-Lievre F, Buck CA. Vasculogenesis in the early quail blastodisc as studied with a monoclonal antibody recognizing endothelial cells. Development. 1987; 100:339–349. [PubMed: 3308401]
53. Ramirez-Bergeron DL, Simon MC. Hypoxia-inducible factor and the development of stem cells of the cardiovascular system. Stem Cells. 2001; 19:279–286. [PubMed: 11463947]
54. Ramirez-Bergeron DL, Runge A, Adelman DM, Gohil M, Simon MC. HIF-dependent hematopoietic factor regulate the development of the embryonic vasculature. Dev Cell. 2006; 11:81–92. [PubMed: 16824955]
55. Reese DE, Mikawa T, Bader DM. Development of the coronary vessel system. Circ Res. 2002; 91:761–768. [PubMed: 12411389]
56. Richard DE, Berra E, Pouyssegur J. Nonhypoxic pathway mediates the induction of hypoxia-inducible factor 1 alpha in vascular smooth muscle cells. J Biol Chem. 2000; 275:26765–26771. [PubMed: 10837481]
57. Ryan HE, Lo J, Johnson RS. HIF-1α is required for solid tumor formation and embryonic vascularization. EMBO J. 1998; 17:3005–3015. [PubMed: 9606183]
58. Sakurai Y, Ohgimoto K, Kataoka Y, Yoshida N, Shibuya M. Essential role of flk-1 (VEGF receptor 2) tyrosine residue 1173 in vasculogenesis in mice. Proc Natl Acad Sci USA. 2005; 102:1076–1081. [PubMed: 15644447]
59. Sallee D, Qiu Y, Liu J, Watanabe M, Fisher SA. Fas ligand gene transfer to the embryonic heart induces programmed cell death and outflow tract defects. Dev Biol. 2004; 267:309–319. [PubMed: 15013796]
60. Semenza GL, Wang G. A nuclear factor induced by hypoxia via de novo protein synthesis binds to the human erythropoietin gene enhancer at a site required for transcriptional activation. Mol Cell Biol. 1992; 12:5447–5454. [PubMed: 1448077]
61. Semenza GL, Jiang B, Leung S, Passantino R, Concordet J, Maire P, Giallongo A. Hypoxia response elements in the aldolase A, enolase 1, and lactate dehydrogenase A gene promoters contain essential binding sites for hypoxia-inducible factor 1. J Biol Chem. 1996; 271:32529–32537. [PubMed: 8955077]
62. Semenza GL. HIF-1 and mechanisms of hypoxia sensing. Curr Opin Cell Biol. 2001; 13:167–171. [PubMed: 11248550]
63. Semenza GL. Targeting HIF-1 for cancer therapy. Nat Rev Cancer. 2003; 3:721–732. [PubMed: 13130303]
64. Semenza GL. Hydroxylation of HIF-1: Oxygen sensing at the molecular level. Physiology. 2004; 19:176–182. [PubMed: 15304631]
65. Sheikh AY, Gibson JJ, Rollins MD, Hopf HW, Hussain Z, Hunt TK. Effect of hyperoxia on vascular endothelial growth factor levels in a wound model. Arch Surg. 2000; 135:1293–1297. [PubMed: 11074883]
66. Shyu KG, Wang MT, Wang BW, Chang CC, Leu JG, Kuan P, Chang H. Intramyocardial injection of naked DNA encoding HIF-1a/VP16 hybrid to enhance angiogenesis in an acute myocardial infarction model in the rat. Cardiovasc Res. 2002; 54:576–583. [PubMed: 12031703]
67. Sugishita Y, Watanabe M, Fisher SA. Role of myocardial hypoxia in the remodeling of the embryonic avian cardiac outflow tract. Dev Biol. 2004A; 267:294–308. [PubMed: 15013795]
68. Sugishita Y, Leifer D, Watanabe M, Agani F, Fisher SA. Hypoxia-responsive ignaling regulates the apoptosis-dependent remodeling of the embryonic avian cardiac outflow tract. Dev Biol. 2004B; 273:285–296. [PubMed: 15328013]
69. Sugishita Y, Watanabe M, Fisher SA. The development of the embryonic outflow tract provides novel insights into cardiac differentiation and remodeling. Trends Cardiovasc Med. 2004C; 14:235–241. [PubMed: 15451515]
70. Taylor AJ, Rogan KM, Virmani R. Sudden cardiac death associated with isolated congenital coronary artery anomalies. J Am Coll Cardiol. 1992; 20:640–647. [PubMed: 1512344]
71. Tomanek RJ. Formation of the coronary vasculature during development. Angiogenesis. 2005; 8:273–284. [PubMed: 16308734]

72. Tomanek RJ, Ishii Y, Holifield JS, Sjogren CL, Hansen HK, Mikawa T. VEGF family members regulate myocardial tubulogenesis and coronary artery formation in the embryo. Circ Res. 2006A; 98:947–953. [PubMed: 16527987]
73. Tomanek RJ, Hansen HK, Dedkov EI. Vascular patterning of the quail coronary system during development. Anat Rec A Discov Mol Cell Evol Biol. 2006B; 288:989–999. [PubMed: 16892426]
74. Tomanek RJ, Hansen HK, Christensen LP. Temporally expressed PDGF and FGF-2 regulate embryonic coronary artery formation and growth. Arterioscler Thromb Vasc Biol. 2008; 28:1237–1243. [PubMed: 18420995]
75. Turcotte S, desrosiers RR, Beliveau R. HIF-1 alpha mRNA and protein upregulation involves RhoGTPase expression during hypoxia in renal cell carcinoma. J Cell Sci. 2003; 116:2247–2260. [PubMed: 12697836]
76. Ushio-Fukai M, Alexander RW. Reactive oxygen species as mediators of angiogenesis signaling: Role of NAD(P)H oxidase. Mol Cell Biochem. 2004; 264:85–97. [PubMed: 15544038]
77. Ushio-Fukai M, Tang Y, Fukai T, Dikalov S, Ma Y, Fujimoto M, Quinn MT, Pagano PJ, Johnson C, Alexander RW. Novel role of gp91phox-containing NAD(P)H oxidase in vascular endothelial growth factor-induced signaling and angiogenesis. Circ Res. 2002; 91:1160–1167. [PubMed: 12480817]
78. Van den Akker NM, Lie-Venema H, Maas S, Eralp I, DeRuiter MC, Poelmann RE, Gittenberger-de Groot AC. Platelet-derived growth factors in the developing avian heart and maturating coronary vasculature. Dev Dyn. 2005; 233:1579–1588. [PubMed: 15973731]
79. van Wetering S, van Buul JD, Quik S, Mul FP, Anthony EC, ten Klooster JP, Collard JG, Hordijk PL. Reactive oxygen species mediate Rac-induced loss of cell-cell adhesion in primary human endothelial cells. J Cell Sci. 2002; 115:1837–1846. [PubMed: 11956315]
80. Vincent KA, Shyu KG, Luo Y, Magner M, Tio RA, jiang C, Goldberg MA, Akita GY, Gregory RJ, Isner JM. Angiogenesis is induced in a rabbit model of hindlimb ischemia by naked DNA encoding an HIF-1a/VP16 hybrid transcription factor. Circulation. 2000; 102:2255–2261. [PubMed: 11056102]
81. Waldo KL, Willner W, Kirby ML. Origin of the proximal coronary artery stems and a review of ventricular vascularization in the chick embryo. Am J Anat. 1990; 188:109–120. [PubMed: 2375277]
82. Waldo KL, Kumiski DH, Kirby ML. Association of the cardiac neural crest with development of the coronary arteries in the chick embryo. Anat Rec. 1994; 239:315–331. [PubMed: 7943763]
83. Wang GL, Jiang BH, Semenza GL. Effect of altered redox states on expression and DNA-binding activity of hypoxia-inducible factor 1. Biochem Biophys Res Commun. 1995; 212:550–556. [PubMed: 7626069]
84. Watanabe M, Choudhry A, Berlan M, Singal A, Siwik E, Mohr S, Fisher SA. Developmental remodeling and shortening of the cardiac outflow tract involves myocyte programmed cell death. Development. 1998; 125:3809–3820. [PubMed: 9729489]
85. Watanabe M, Jafri A, Fisher SA. Apoptosis is required for the proper formation of the ventriculo-arterial connections. Dev Biol. 2001; 240:274–288. [PubMed: 11784063]
86. Wikenheiser J, Doughman YQ, Fisher SA, Watanabe M. Differential levels of tissue hypoxia in the developing chicken heart. Dev Dyn. 2006; 235:115–123. [PubMed: 16028272]
87. Witmer AN, Vrensen GF, Van Noorden CJ, Schlingemann RO. Vascular endothelial growth factors and angiogenesis in eye disease. Prog Retin Eye Res. 2003; 22:1–29. [PubMed: 12597922]
88. Xu B, Doughman Y, Turakhia M, Jiang W, Landsettle CE, Agani FH, Semenza GL, Watanabe M, Yang YC. Partial rescue of defects in Cited2-deficient embryos by HIF-1alpha heterozygosity. Dev Biol. 2007; 301:130–40. [PubMed: 17022961]
89. Yamakawa M, Liu LX, Date T, Belanger AJ, Vincent KA, Akita GY, Kuriyama T, Cheng SH, Gregory RJ, Jiang C. Hypoxia-inducible factor-1 mediates activation of cultured vascular endothelial cells by inducing multiple angiogenic factors. Circ Res. 2003; 93:664–673. [PubMed: 12958144]
90. Yang ZZ, Zhang AY, Yi FX, Li PL, Zou AP. Redox regulation of HIF-1 alpha levels and HO-1 expression in remal medullary interstitial cells. Am J Physiol Renal Physiol. 2003; 284:F1207–F1215. [PubMed: 12595275]

91. Zachary I. Neuroprotective role of vascular endothelial growth factor: signaling mechanisms, biological function, and therapeutic potential. Neurosignals. 2005; 14:207–221. [PubMed: 16301836]

92. Zhang L. Prenatal hypoxia and cardiac programming. J Soc Gynecol Investig. 2005; 12:2–13.

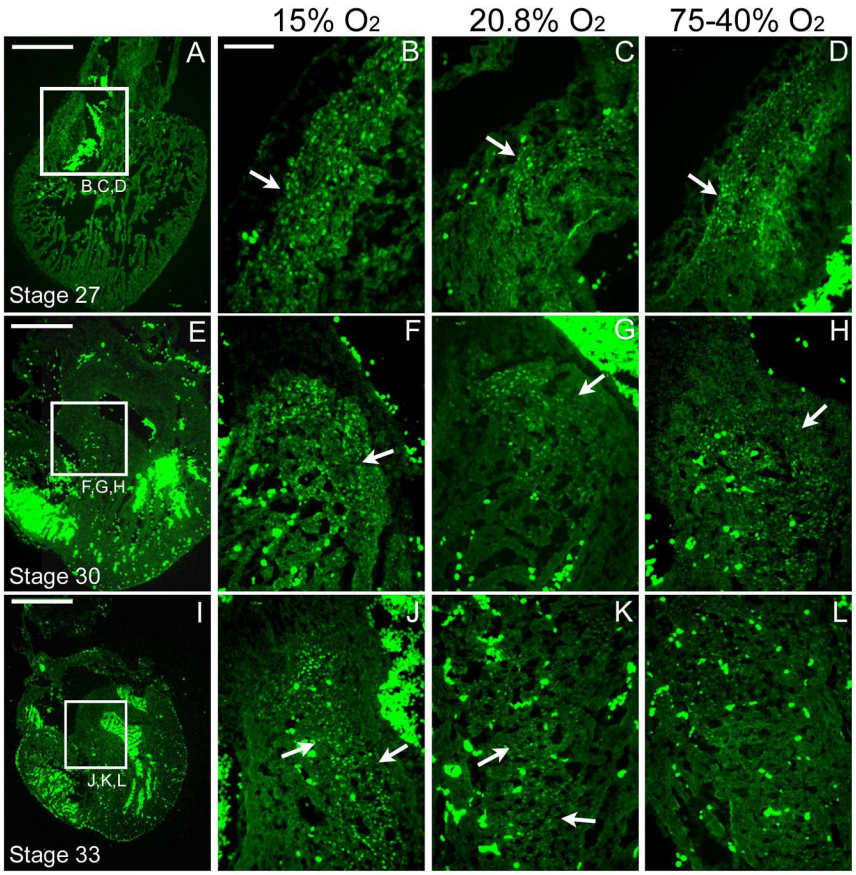

Figure 1. HIF-1α positive staining in the frontal plane at stage 27, 30 & 33 under altered ambient oxygen levels

A, **E** and **I** are low-magnification normoxic controls. **A–D** are images at the outflow tract of a stage 27 (ED 5.5) embryo exposed to hypoxic (15% O_2), normoxic (20.8% O_2) and hyperoxic (75-40% O_2) conditions (**B–D** respectively). **E–H** are images at the interventricular septum of a stage 30 (ED 6.5) embryo exposed to hypoxic, normoxic and hyperoxic conditions (**F–H** respectively). **I–L** are images near the interventricular septum of a stage 33 (ED 7.5) embryo exposed to hypoxic, normoxic and hyperoxic conditions (**J–L** respectively). Arrows indicate the location of HIF-1α staining. The bright green staining within the ventricular lumens is the autofluorescence of red blood cells. Negative controls not shown. Scale bar = 500 μm in **A**, **E** and **I**. The scale bar in **B** = 100 μm (applies to **B–D**, **F–H**, and **J–L**).

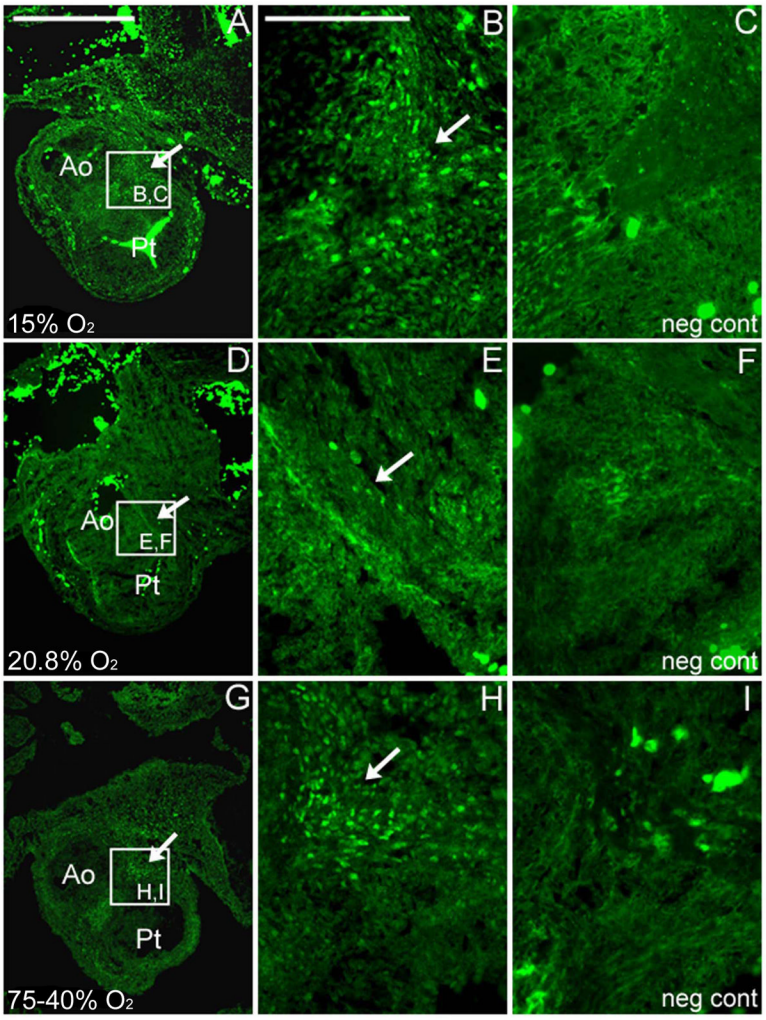

Figure 2. HIF-1α positive staining of the outflow tract in the transverse plane at stage 30 under altered ambient oxygen levels

This specific region of the OFT is at the level of the future site of left and right coronary attachments to the aorta. Under both hypoxia (**A, B**) and hyperoxia (**G, H**) conditions, there was an increase in the number of cells with HIF-1α nuclear staining compared to the normoxic controls (**D, E**). Arrows indicate cells with HIF-1α nuclear staining. No nuclear staining was observed in the negative control sections from the same region (neg cont; **C, F, I**) stained in parallel with no first antibody added. Scale bar = 100 μm in **A** (applies to **A, D** and **G**). The scale bar in **B** = 50 μm (applies to **B–C, E–F,** and **H–I**). Ao, aorta; Pt, pulmonary trunk.

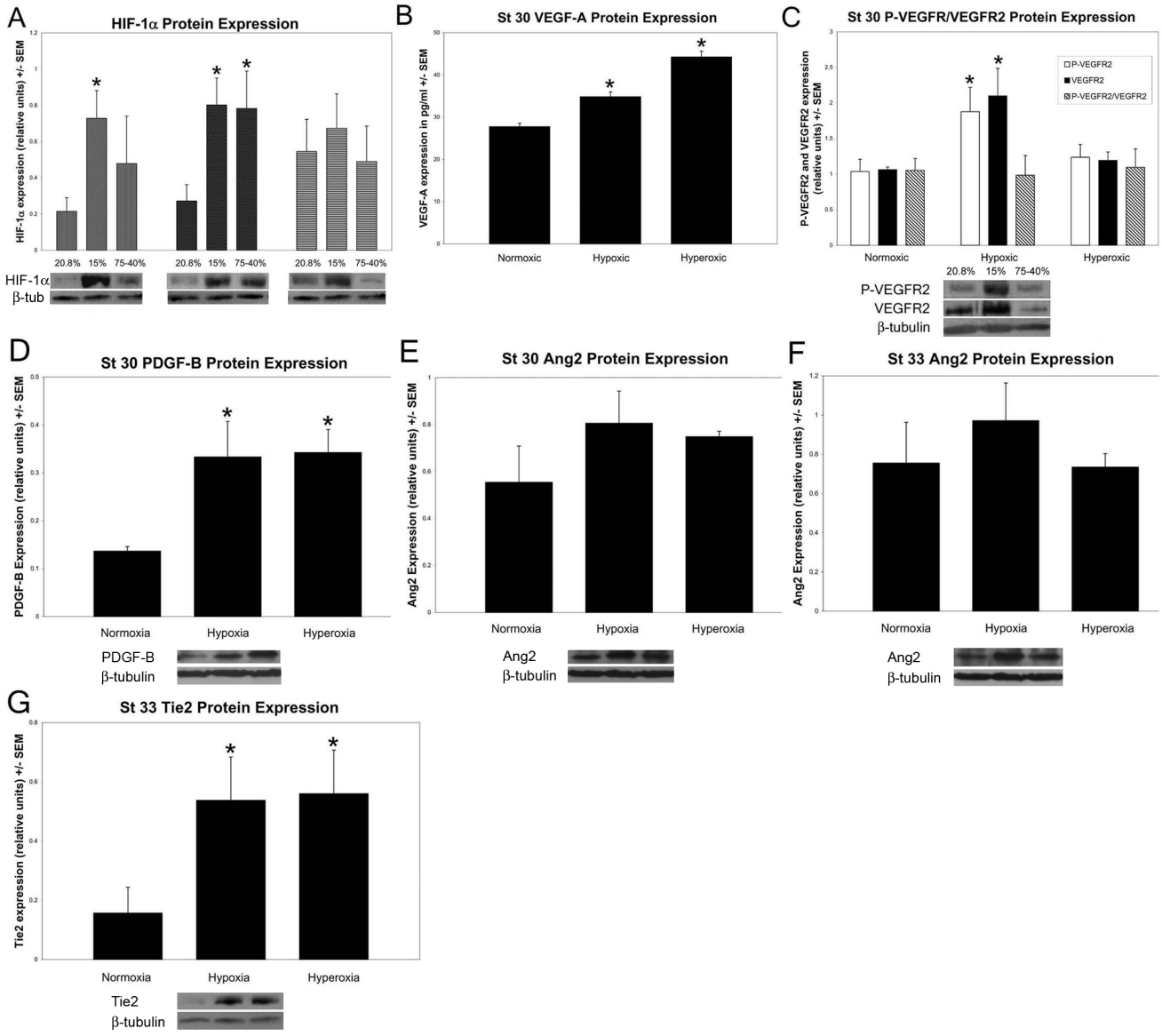

Figure 3. Protein expression of HIF-1α and select downstream targets under the hypoxic and hyperoxic regimens

HIF-1α, PDGF-B, Ang2 and Tie2 protein expression was analyzed by Western blot. VEGF-A was analyzed by ELISA and VEGFR2 by immunoprecipitation. **A**: HIF-1α protein expression from stages 27, 30 and 33 after exposure to hypoxic and hyperoxic regimens compared to HIF-1α basal levels detected in extracts from embryos exposed to ambient (normoxic) oxygen control levels. HIF-1α protein expression was significantly higher than control levels under hypoxia at both stage 27 and 30 ($n = 6$) (St 27 p = 0.009; St 30 p = 0.005). Unexpectedly, HIF-1α protein expression was also significantly higher under hyperoxic conditions at stage 30 (p = 0.03). **B**: VEGF-A was significantly increased under both hypoxic and hyperoxic regimens at stage 30 ($n = 4$) (p = 0.003, p = 0.002 respectively). **C**: Phosphorylated-VEGFR2 and total VEGFR2 were significantly increased under only the hypoxic regimen at stage 30 ($n = 4$) (p = 0.01; p = 0.01 respectively). The ratio of the levels of phosphorylated VEGFR2 compared to total VEGFR2 was consistent over the 3 conditions at stage 30. **D**: PDGF-B was significantly increased under both hypoxic and

hyperoxic regimens at stage 30 ($n = 4$) (p = 0.01, p = 0.01 respectively). **E**: Stage 30 Ang2 expression was upregulated under both hypoxia and hyperoxia but not to a significant level ($n = 4$). **F**: Stage 33 Ang2 expression one-half day after the left and right coronary arteries attached to the aorta. Similar to results from stage 30 extracts, there was no significant increase under either the hypoxic or hyperoxic regimens ($n = 4$). **G**: Stage 33 Tie2 expression was significantly increased under both hypoxia and hyperoxia ($n = 4$) (p = 0.01; p = 0.01 respectively).

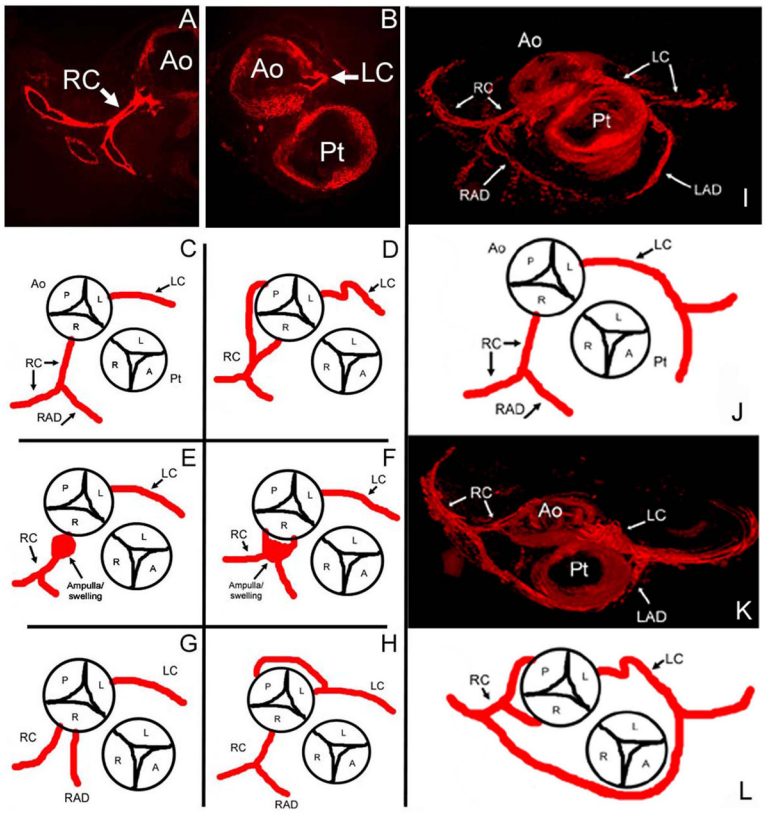

Figure 4. Diagrams and 3D imaging of stage 35 coronary artery anomalies

A and **B** are stage 35 (ED 9) α-smooth muscle actin stained proximal coronary arteries near the base of the aorta in the transverse plane of an embryo exposed to normoxic conditions. **C–H** are diagrams of the route of the proximal coronary arteries detected by observation of serial transverse sections stained as in A and B of this region for α-smooth muscle actin. **C** is the route of the proximal coronary arteries in a control embryo (n = 10). **D–H** are anomalies observed in embryos incubated under the hypoxic regimen (n = 9/10). **D** has a right coronary originating from the posterior cusp in addition to a coronary originating from the right cusp. There is also a tortuous left coronary (LC, arrow). **E** and **F** displayed a swelling near the right coronary attachment to the aorta. **G** had double right coronaries originating from the right cusp. **H** displayed a retro-aortic branch originating from the left coronary artery and connecting to the posterior cusp. Hyperoxic embryos had anomalies (n = 5/10) that included **H** (4/10) and **G** (1/10). Ao, aorta; Pt, pulmonary trunk; LC, left coronary artery; RC, right coronary artery, RAD, right anterior descending artery (conotruncus branch); A, P, L and R = anterior, posterior, left and right cusps. AMIRA® software was used to 3D reconstruct stage 35 (ED 9) embryos for verification of coronary artery morphology we noted in stained serial sections (**A, B**). **A** is a normoxic control. **B** is an embryo exposed to 15% O_2 from stages 25–35 (ED 4.5-9). This particular embryo displays a tortuous left coronary and double right coronaries, one which attaches at the posterior cusp. Note the altered angles of the right coronary and anastamosing arteries located very close to the pulmonary trunk. **C** is a diagram depicting figure **A. D** is a diagram depicting **B**. Ao, aorta; Pt, pulmonary trunk; LC, left coronary artery; RC, right coronary artery; LAD, left anterior descending artery; RAD, right anterior descending artery (conotruncus branch); A, P, L and R = anterior, posterior, left and right cusps.

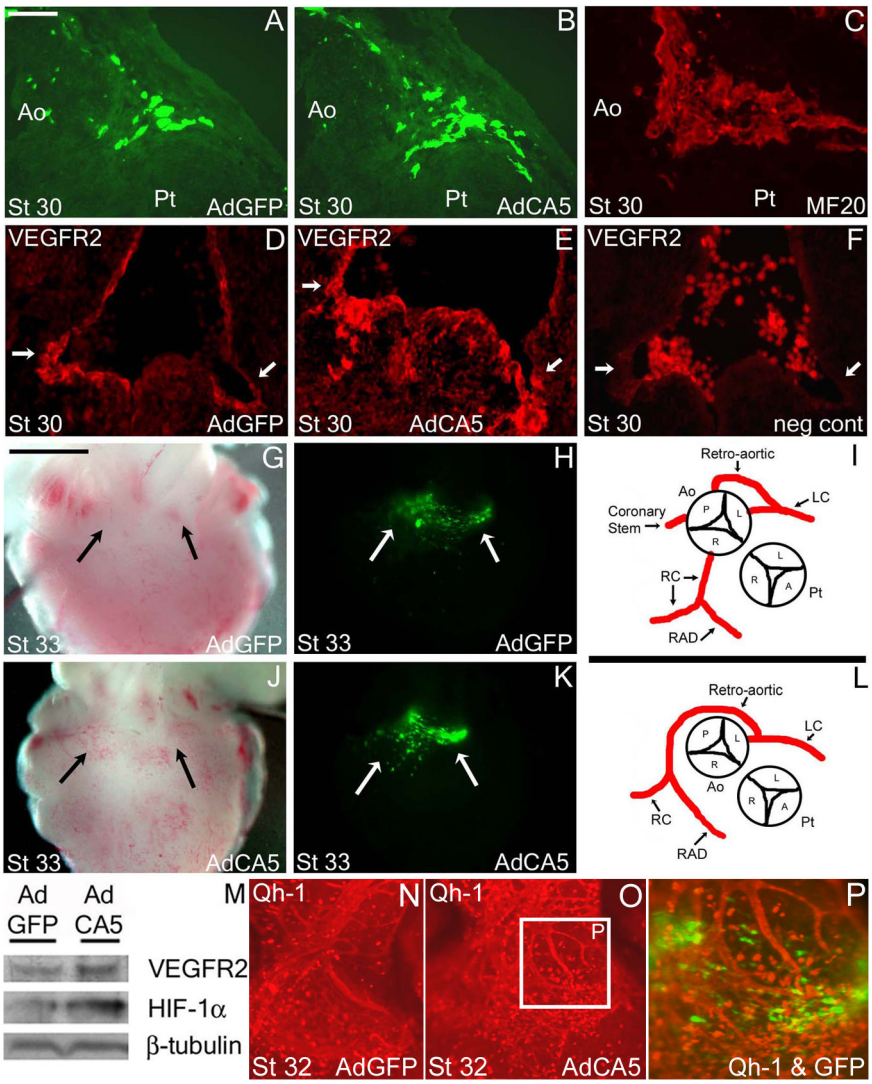

Figure 5. GFP expression after injection of a constitutively active form of HIF-1α (AdCA5) and control (AdGFP) adenoviruses

Both the AdCA5 and control (AdGFP) injected embryos had green fluorescent protein (GFP) expression at the base of the OFT in the myocardium. **A–C**: GFP was expressed adjacent to the site of future attachment of the left coronary artery to the aorta at embryonic day 6.5 (stage 30) (**A, B**). MF20 immunostaining indicated that GFP expression is located in cardiomyocytes (**C**). **D–F**: Frontal plane VEGFR2 positive staining near the future attachments of the left and right coronary arteries, with a stronger and broader region of immunostaining after AdCA5 injection (**E**). Negative control for VEGFR2 staining with no first antibody added (**F**). **G, H, J, K**: Wholemount images of AdGFP and AdCA5 infected embryo hearts under brightfield (**G, J**) and fluorescence activation (**H, K**) near the base of the outflow tract where the coronary arteries have attached to the aorta (arrows). (**I, L**) Coronary anomalies of the left and right coronary arteries after injection of AdCA5 included retro-aortic branches to/from the left coronary artery, retro-aortic branches that travel along the route of the right coronary artery and extra coronary stems connected to the aorta. These are similar to anomalies seen in embryos incubated under hypoxic and hyperoxic regimens. **M**: Protein expression in whole heart extracts of HIF-1α and VEGFR2 after injection of

AdGFP and AdCA5 adenoviruses at stage 30. The quail embryo OFT myocardium was infected with control AdGFP adenovirus (**N**) or AdCA5 adenovirus (**O**, **P**) at stage 17 and harvested at stage 32. A higher density of single Qh-1+ cells (red) were found at the base of the OFT compared with control embryos. Qh-1+ vessels adjacent to cells expressing AdCA5 (green) differed in pattern. Qh1+ cells (red) are not the GFP+ cells transduced with adenovirus expressing AdCA5 (overlay, **P**). Scale bar = 25 μm in **A–F**. The scale bar in **B** = 1000 μm (applies to **G, H, J, L**).

Table 1

Coronary anomalies seen under hypoxic, hyperoxic and AdCA5 treatments.

Anatomical Anomalies

Treatment	Anomaly	Rate of occurrence
Hypoxia *n* = 10	2x RC coming off R cusp	4 of 10
	Retro-aortic LC fusing with post cusp region	4 of 10
	Displaying both LC and RC anomalies	4 of 10
	Tortuous LC	2 of 10
	Formation of swellings near RC	2 of 10
	RC coming off posterior cusp	1 of 10
Normoxia *n* = 10	no coronary anomalies	0 of 10
Hyperoxia *n* = 10	Retro-aortic LC fusing with post cusp region	4 of 10
	2x RC coming off R cusp	1 of 10
AdCA5 *n* = 8	Retro-aortic LC fusing with post cusp region	3 of 8
	Extra coronary stem lateral to RC	2 of 8
	Retro-aortic fusing with LC (not a branch of LC)	1 of 8
AdGFP *n* = 8	no coronary anomalies	0 of 8

Anomalies were detected in a total of 90% (9/10) of the embryos incubated under the hypoxic regimen, 50% (5/10) under hyperoxia and 75% (6/8) after injection of the AdCA5. No anomalies were observed in 10 embryos incubated under normoxic conditions and in 8 AdGFP-infected control embryos. Rate of occurrence describes what anomalies were observed and how many existed under a particular treatment. LC = left coronary, RC = right coronary.